Psychoneuroendocrinology 72 (2016) 22–33

Contents lists available at ScienceDirect

Psychoneuroendocrinology

journal homepage: www.elsevier.com/locate/psyneuen

Juvenile exposure to a high fat diet promotes behavioral and limbic alterations in the absence of obesity

Angeles Vinuesa[a,b], Carlos Pomilio[a,b], Martin Menafra[c], Maria Marta Bonaventura[b], Laura Garay[b], María Florencia Mercogliano[b], Roxana Schillaci[b], Victoria Lux Lantos[b], Fernando Brites[c], Juan Beauquis[a,b], Flavia Saravia[a,b,*]

[a] Neurobiology of Aging, Departamento de Química Biológica, Facultad de Ciencias Exactas y Naturales, Universidad de Buenos Aires, Argentina
[b] Instituto de Biología y Medicina Experimental, CONICET, Buenos Aires, Argentina
[c] Facultad de Farmacia y Bioquímica, Universidad de Buenos Aires, Buenos Aires, Argentina

ARTICLE INFO

Article history:
Received 27 January 2016
Received in revised form 3 June 2016
Accepted 4 June 2016

Keywords:
High fat diet
Hippocampal neuroinflammation
Neurogenesis
Periadolescence
Cognitive performance
Emotionality

ABSTRACT

The incidence of metabolic disorders including obesity, type 2 diabetes and metabolic syndrome have seriously increased in the last decades. These diseases – with growing impact in modern societies – constitute major risk factors for neurodegenerative disorders such as Alzheimer's disease (AD), sharing insulin resistance, inflammation and associated cognitive impairment. However, cerebral cellular and molecular pathways involved are not yet clearly understood. Thus, our aim was to study the impact of a non-severe high fat diet (HFD) that resembles western-like alimentary habits, particularly involving juvenile stages where the brain physiology and connectivity are in plain maturation. To this end, one-month-old C57BL/6J male mice were given either a control diet or HFD during 4 months. Exposure to HFD produced metabolic alterations along with changes in behavioral and central parameters, in the absence of obesity. Two-month-old HFD mice showed increased glycemia and plasmatic IL1β but these values normalized at the end of the HFD protocol at 5 months of age, probably representing an acute response that is compensated at later stages. After four months of HFD exposure, mice presented dyslipidemia, increased Lipoprotein-associated phospholipase A2 (Lp-PLA2) activity, hepatic insulin resistance and inflammation. Alterations in the behavioral profile of the HFD group were shown by the impediment in nest building behavior, deficiencies in short and mid-term spatial memories, anxious and depressive-like behavior. Regarding the latter disruptions in emotional processing, we found an increased neural activity in the amygdala, shown by a greater number of c-Fos+ nuclei. We found that hippocampal adult neurogenesis was decreased in HFD mice, showing diminished cell proliferation measured as Ki67+ cells and neuronal differentiation in SGZ by doublecortin labeling. These phenomena were accompanied by a neuroinflammatory and insulin-resistant state in the hippocampus, depicted by a reactive phenotype in Iba1+ microglia cells (increased in number and soma size) and an impaired response to insulin given by decreased phosphorylated Akt levels and increased levels of inhibitory phosphorylation of IRS1. Our data portray a set of alterations in behavioral and neural parameters as a consequence of an early-life exposure to a quite moderate high fat diet, many of which can resemble AD-related features. These results highly emphasize the need to study how metabolic and neurodegenerative disorders are interrelated in deep, thus allowing the finding of successful preventive and therapeutic approaches.

© 2016 Elsevier Ltd. All rights reserved.

Abbreviations: AD, Alzheimer's disease; CD, control diet; DCX, doublecortin; DG, dentate gyrus; EPM, elevated plus maze; GCL, granular cell layer; HFD, high fat diet; HPA, hypothalamic-pituitary-adrenal axis; Iba1, ionized calcium binding adapter molecule 1; IL1β, interleuquin 1 β; IRS, insulin receptor substrate; Lp-PLA2, Lipoprotein-associated phospholipase A2; NB, nest building; NOL, novel object location recognition test; SGZ, subgranular zone; T2D, type 2 diabetes; TNFα, tumor necrosis factor α; TST, tail suspension test.

* Corresponding author at: Instituto de Biología y Medicina Experimental, CONICET and Departamento de Química Biológica, Facultad de Ciencias Exactas y Naturales, Universidad de Buenos Aires, Obligado 2490-1428, Buenos Aires, Argentina.
E-mail addresses: fsaravia@qb.fcen.uba.ar, fesaravia@gmail.com (F. Saravia).

http://dx.doi.org/10.1016/j.psyneuen.2016.06.004
0306-4530/© 2016 Elsevier Ltd. All rights reserved.

1. Introduction

Recent data from the World Health Organization (WHO) revealed an alarming increase of obesity and overweight, responsible for more deaths than underweight in high and middle income countries. The number of obese patients has been duplicated in the last decades in the world and, regrettably, this increase has been even higher within the infant population (WHO, 2015). The over-consumption of industrialized food with a high content of fat is directly implicated, in addition to changes in lifestyle that include low physical activity. During the juvenile period, feeding habits and especially food quality can potentially impact on behavior, emotionality and cognitive capabilities during adulthood, increasing the risk to develop neurodegenerative diseases in both, humans and animal models (Vendruscolo et al., 2010; Andersen, 2003).

Obesity, insulin resistance and type 2 diabetes (T2D) are major consequences of modern feeding habits and their effects on the central nervous system are thought to be mediated through multiple pathways. Obesity and high fat diet consumption are associated with dyslipidemia and alterations in cholesterol levels contributing to inflammation and pro atherogenic status via high oxidative stress. Obesity-associated peripheral and brain inflammatory processes promote the development of emotional and cognitive alterations, (reviewed in Castanon et al., 2015). Furthermore, increased levels of inflammatory cytokines as TNFα can contribute to central and peripheral insulin signaling dysfunction, aggravating the scene (Miller and Spencer, 2014).

As our group and others have shown, neuroinflammation is found in metabolic disorders. Activation of hippocampal astrocytes and microglia are common findings in spontaneous models of type 1 and type 2 diabetes (Beauquis et al., 2006, 2008, 2010; Biessels et al., 1994). Due to its high glucose demand and elevated insulin sensitivity, the hippocampus can participate in central insulin resistance and subsequently promote brain aging and age-related illnesses as Alzheimer's disease (Dineley et al., 2014; Fehm et al., 2006). The amygdala and the hippocampus are recognized as stress-sensitive structures that experience decisive changes during the adolescent period (LeDoux, 2003; Maren, 2005). Thus, metabolic disturbances with a juvenile onset can interfere with limbic maturation and induce lifelong cognitive and emotional alterations.

Multiple lines of evidence from clinical and epidemiological studies indicate that overweight and obesity are growing global public health problems recognizing multifactorial contributions including genetic, behavioral and environmental agents. A number of different risk factors are shared by T2D, cardiovascular pathology and hypertension; moreover, these pathologies are also associated with neurological and psychological outcomes, being among them impulsivity, attention-deficit hyperactivity disorder, depression and anxiety (Puder and Munsch, 2010).

Obesity and insulin signaling defects have been shown to be associated with brain disorders (de la Monte and Tong, 2014; Freeman et al., 2014; Moll and Schubert, 2012) Mice rendered diabetic (Beauquis et al., 2006) and also genetic models show alterations in synaptic transmission, adult neurogenesis, behavior and glial support and reactivity (Beauquis et al., 2008, 2010; Calvo-Ochoa and Arias, 2015; Stranahan et al., 2008). These issues highlight the importance of searching common cellular and molecular pathways in order to design preventive and therapeutic strategies.

The purpose of this work was to study neural and behavioral effects of a non-severe high fat diet in mice – that could be assimilated to a modern western diet – administered during the critical juvenile stage, focusing on limbic structures, cognitive performance and emotionality. Our hypothesis considers that the exposure to a high fat diet during a susceptible period of the early life may influence brain plasticity. In particular, alterations in hippocampal neurogenic capability could potentially increase the risk to develop cognitive failure or anxiety symptoms, common to diseases like depression and dementia.

Our results show that the exposure to a moderately high fat diet during the juvenile period failed to induce significant overweight and hyperglycemia but was sufficient to provoke relevant peripheral and central changes in adulthood. These alterations could represent premature signs of neurological diseases. Though obesity and overt diabetes are frequently diagnosed, other metabolic disorders could have a subclinical course, constituting 'silent' cardiovascular and brain disease risk factors that are usually present since an early age. Therefore, the normoglycemic non-obese mouse model that we describe in the present study may help to improve diagnosis and prevent CNS complications in the context of subclinical metabolic disorders as well as contributing to the study of the pathways involved.

2. Material and methods

2.1. Animals and diets

C57BL/6J mice (Jackson Laboratories, Bar Harbor, ME) were maintained in our animal facility (Institute of Biology and Experimental Medicine, CONICET; NIH Assurance Certificate # A5072-01) and were housed under controlled conditions of temperature (22 °C) and humidity (50%) with 12 h/12 h light/dark cycles (lights on at 7:00 am). All animal experiments followed the NIH Guide for the Care and Use of Laboratory Animals and were approved by the Ethics Committee of the Institute of Biology and Experimental Medicine. All efforts were done to reduce the number of mice used in the study as well as to minimize animal suffering and discomfort.

One month-old male mice were exposed to control or a high fat diet during four months, as the experimental scheme shows (Fig. 1A). Both control diet (CD) and high fat diet (HFD) were provided by Gepsa Feeds (Grupo Pilar, Pilar, Buenos Aires, Argentina). CD pellets provided 2.5 kcal/g energy and were composed by: carbohydrate 28.8%, proteins 25.5%, fat 3.6%, fibers 27.4%, minerals 8.1% and humidity 6.7%. HFD pellets were custom-prepared and provided 3.9 kcal/g energy. HFD pellets' composition included: carbohydrate 22.5%, proteins 22.8%, fat 21.1%, fibers 23.0%, minerals 5.6% and humidity 5.0%. The main fat components of HFD pellets were monounsaturated fatty acids (44.7%), saturated fatty acids (29.8%) and polyunsaturated fatty acids (20.9%), among others as it was reported by Valdivia et al. (2014) using this diet. The ratio between omega 3/omega 6 polyunsaturated fatty acids did not differ comparing HFD to CD and the ratio value was near 17 in both diets.

Thirty five mice were used in total, comprising 15 CD and 20 HFD mice. During the last month of exposure to the diet, the behavioral profile was assessed as described in Section 2.1 and euthanasia was done 5–7 days after the last behavioral task was performed. At end point, the procedure was as follows: CD and HFD mice were fasted for 6-h (fasting started one hour after lights on), weighed, glucose was measured from tail blood, anesthetized with ketamine (IP 80 mg/kg BW, Holliday-Scott, Argentina) and xylazine (IP 10 mg/kg BW, Bayer, Argentina), stimulated for ten minutes with insulin (IP 5 UI/kg BW, Beta Laboratory, Argentina) and then decapitated.

Additionally, a different group of 20 animals was exposed to either CD or HFD (n = 10 for each group) and euthanized at two months of age in order to assess certain parameters, such as weight, glycemia and inflammatory markers.

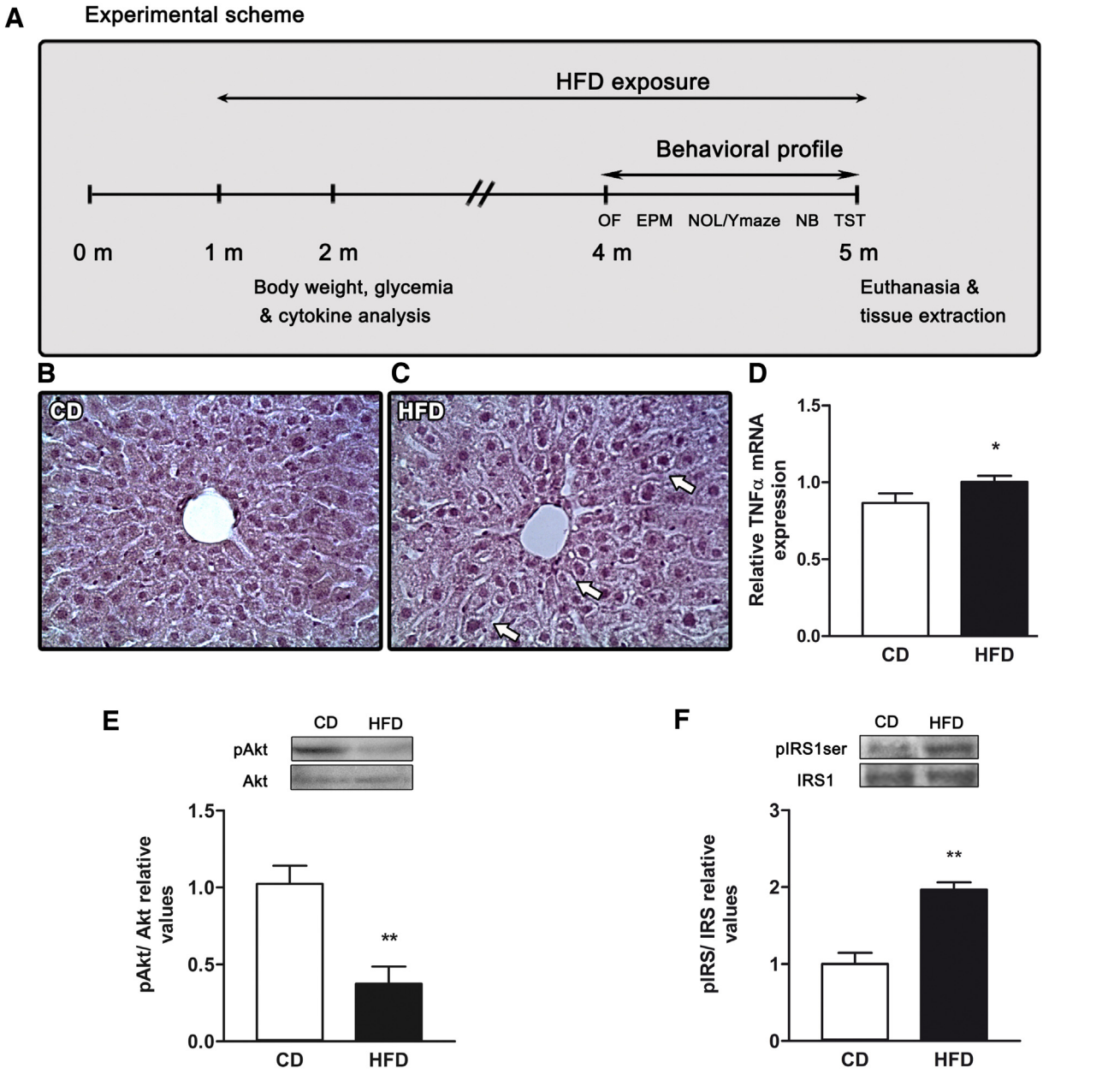

Fig. 1. Experimental scheme and liver alterations induced by HFD exposure. One month-old male mice were exposed either to CD or HFD ad libitum until the age of 2 or 5 months. Weight and food consumption were assessed weekly. During the last month of exposure to the diet (fifth month), the behavioral tasks were performed and afterwards euthanasia and tissue processing took place (A). Paraffin embedded liver sections stained with H&E (B and C) show perinuclear blank spaces marked with white arrows in HFD hepatocytes. In (D) the graph shows liver TNFα expression measured by RT-qPCR. Panels (E) and (F) show representative western blot bands corresponding to liver protein levels of total Akt and IRS1 levels and their phosphorylated states in CD and HFD groups with the corresponding densitometry analysis. Data is expressed as pAkt/Akt or pIRS1/IRS1 densitometry ratio relative to CD ratio. (Student's *t*-test for independent samples, * $p < 0.05$, ** $p < 0.01$). For interpretation of the references to color in this figure legend, the reader is referred to the web version of the article.

2.2. Tissue processing

Trunk blood was collected, centrifuged at 12000*g* for 20 min, 4 °C and serum stored at −20 °C for metabolic determinations. Liver was quickly extracted; one lobule was frozen in dry ice and stored at −80 °C until use for protein and mRNA expression analysis, and a second lobule was fixed overnight in 4% paraformaldehyde solution at 4 °C, properly ethanol dehydrated, xylene cleared and paraffin embedded for sectioning at 10 μm in a rotatory microtome. Pancreas was rapidly extracted, frozen in dry ice and stored at −80 °C until use for determination of insulin content.

Brains were removed from the skull and both hemispheres differently processed. The hippocampus was dissected form the left hemisphere, frozen in dry ice and stored at −80 °C until use. A subgroup of frozen hippocampi was processed for RT-qPCR, another one for immunoblotting and the third one for ELISA determinations. Hippocampi that was used for western blot or ELISA was homogenized in supplemented RIPA buffer and those used for RT-qPCR were processed with trizol reagent as further detailed. The right hemisphere was fixed overnight in a 4% paraformaldehyde solution at 4 °C and then cut coronally at 60 μm in a vibrating microtome (Vibratome 1000P, USA). Sections were stored in a cryoprotectant solution (25% glycerol, 25% ethylene glycol, 50% phosphate buffer 0.1 M, pH 7.4) at −20 °C until use. All immunohistochemical techniques and Cresyl Violet counter-staining were performed on free-floating sections. For cell number and morphometric anal-

yses, six brain sections per mouse were evaluated. In all detailed cases in the following sections, ventral and dorsal hippocampi were considered.

2.3. Cytokines assessment

Mouse TNFα and IL-1β concentrations were measured in animal serum and hippocampal homogenates of 2 or 5-month-CD or HFD mice by ELISA using BD OptEIA™ mouse TNF ELISA Set II kit (catalog number: 558534, BD Biosciences, Franklin Lakes, NJ, USA) and Mouse IL-1βsMini ABTS ELISA Development Kit (catalog number: 900-M47, PreproTech, Rocky Hill, NJ, USA) following the manufacturerís specifications. The experiments were performed in triplicates. The results were obtained with a microplate spectrophotometer.

2.4. Immunohistochemistry

Briefly, after blocking of nonspecific antigenic sites, sections were incubated overnight at 4 °C with the following primary antibodies: rabbit polyclonal anti-Iba1 (1:1500, Wako Pure Chemical Industries, Osaka, Japan), goat polyclonal anti-DCX (1:400, SC-8066, Santa Cruz Biotechnology, USA), rabbit polyclonal anti-Ki67 (1:2000 Novocastra/Leica, Germany) or rabbit polyclonal anti-c-Fos (1:3000, SC-7202, Santa Cruz Biotechnology, USA). We used biotinylated secondary antibodies (1:1000 Vector Laboratories USA) followed by processing with ABC kit (Vector Laboratories) and development with 2 mM diaminobenzidine (Sigma, USA) and 0.5 mM H_2O_2 in 0.1 M Tris buffer. Sections were put on gelatin-coated slides, air-dried overnight, dehydrated in graded solutions of ethanol, cleared in xylene, and mounted with Canada balsam. For image acquisition, Nikon E200 microscope was used.

2.4.1. c-Fos positive nuclei in amygdala

The number of c-Fos immunopositive cells was assessed in the amygdala on brain sections counter-stained with Cresyl violet. Due to the difficulty to state the limits between basolateral and central amygdala in certain sections, we inform the results as the number of c-Fos nuclei in an area including these two subregions, though predominantly representing basolateral amygdala. Nuclei positive for c-Fos was counted under a 40× objective. c-Fos nuclei density (nuclei/mm^2) was quantified analyzing 63,523.02 μm^2 fields in central and basolateral amygdala from each brain section to obtain an average of c-Fos nuclei/mm^2.

2.4.2. Proliferation capability: Ki67 positive cells in the SGZ

Quantification of the number of Ki67+ cells was done under a 40× objective. Cells were counted in both upper and lower blades of the SGZ.

2.4.3. DCX positive neurons in the dentate gyrus

Quantification of the number of DCX+ cells was done as it was previously reported by our group (Beauquis et al., 2014). Cells were counted in the SGZ and in the GCL. Both upper and lower blades of the GCL and SGZ were considered for cell counting.

2.4.4. Microglial density

Microglial density was estimated as it was already reported (Pomilio et al., 2016) using a randomly placed 6×10^5 μm^3 counting probe on two different hippocampal subfields: stratum radiatum and hilus. A minimum of 100 cells per animal was counted.

2.4.5. Microglial soma size

Microphotographs from randomly chosen individual cells in the hippocampal stratum radiatum and hilus were obtained, the soma was delineated and its surface quantified using ImageJ software. At least 50 cells were measured in each animal.

2.5. Metabolic parameters

All metabolic parameters were measured after a 6-h fasting.

2.5.1. Glycemia

Glycemia was measured on tail blood with a glucometer (One Touch Accutrend GC, Boehringer Mannheim, Germany).

2.5.2. Lipid profile

Triglycerides and total cholesterol were quantified by standardized methods (Roche Diagnostics, Mannheim, Germany) in Selectra-2 autoanalyzer. HDL was isolated in the supernatant obtained following precipitation of Apo B-containing lipoproteins with 40 g/L phosphotungstic acid in the presence of magnesium ions.

2.5.3. Lipoprotein-associated phospholipase A2 activity

LpPLA2 activity was measured following the radiometric assay described by Blank et al. (1983) with few modifications (Muzzio et al., 2009). The separation of the released radiolabeled acetate from the lipid substrate was carried out by phase–phase partitioning and measurement of the radioactivity in the aqueous phase. The radioactivity of the aqueous phase was measured by liquid scintillation using a Liquid Scintillation Analyzer (Packard 210TR; Packard Instruments, Meridian, CT). Radioactivity of the substrate-buffer was also measured. Results were expressed as umol/ml.h. Measurements were all carried out within the same assay. Within-run precision (CV) for Lp-PLA2 activity was 5.1%.

2.5.4. Pancreatic insulin content and serum insulin determination

Pancreatic insulin content was measured as previously described (Bonaventura et al., 2008). To measure pancreas insulin content pancreases were weighed, and insulin was extracted from homogenates with acid-ethanol and extracted overnight at 4 °C. Homogenates were centrifuged (10 min, 2000 *g*, 4 °C) and the supernatants neutralized with 0.85 M Tris. After a second incubation (60 min, −20 °C) and centrifugation (30 min, 3000 *g*, 4 °C), the supernatants were stored at −70 °C until used. Pancreatic and serum insulin was measured by RIA using human insulin for iodination and standard, provided by Laboratorios Beta, and anti-bovine insulin antibody (Sigma, St. Louis, MO). All samples were evaluated in the same RIA. The minimum detectable concentration was 2 ng, and the intra-assay coefficient of variation was 6.8%.

2.5.5. HOMA index calculation

Homeostatic model assessment (HOMA), index of insulin resistance was calculated with basal blood glucose and basal insulin measured after 6-h fasting. HOMA-IR = Fasting insulin (mU/L) × Fasting glucose (mg/dl)/405.

2.6. Hematoxylin & eosin staining of liver sections

Briefly, paraffin embedded liver sections on gelatin-coated slides were deparaffinized in xylene, rehydrated in graded ethanol solutions, followed by distilled water. Sections were incubated for two minutes in hematoxylin, rinsed with tap water and then incubated with eosin for one minute. Finally, liver sections were dehydrated in graded solutions of ethanol, cleared in xylene, and mounted with Canada balsam.

2.7. Immunoblotting

Frozen hippocampi and livers were homogenized in supplemented Ripa buffer (1:10 relation tissue to buffer) using a Polytron homogenizer. Protein quantification of the homogenates was obtained by the Bradford standardized method (Bradford, 1976) after lysis with loading buffer 5×, were loaded on 10% or 7.5% acrylamide gels, separated by SDS-PAGE, and then transferred to nitrocellulose membranes. Membranes were blocked with 5% milk or BSA in TBS containing 0.5% Tween-20 (TTBS). Blots were incubated overnight at 4 °C with the antibodies anti-Akt1 pS473 (1:500 Cell Signaling, USA), anti-Akt1 (1:500 Santa Cruz, USA), anti-IRS1 pS636/639 (1:500 Cell Signaling, USA) and anti-IRS1 (1:500 Santa Cruz, USA). After initial probing with primary antibodies, membranes were washed in 0.5% TBST and TBS solutions, incubated for 1 h with 1:1000 dilutions of species-appropriate, HRP-conjugated secondary antibodies (Santa Cruz, USA). After washing, immunoreactivity was visualized by reaction in ECL detection reagents (luminol and *p*-coumaric acid; Sigma-Aldrich Co., St. Louis, MO, USA) for 3 min, followed by immediate exposure of the blot in a G-Box (Syngene, UK). Bands at the relevant molecular weights were quantified using the ImageJ plugin for gel analysis.

2.8. Real-time PCR of TNFα

Hippocampi and liver tissues were homogenized in Trizol reagent (Life Technologies-Invitrogen, CA, USA) with a Polytron homogenizer and total RNA was extracted as recommended by the manufacturer. The concentration and purity of total extracted RNA were determined by measuring the optical density of the samples at 260 and 280 nm in a Nanodrop 2000 (Thermo Scientific USA). cDNA templates for PCR amplification were synthesized from 1 μg of total RNA using a MMLV High Performance Reverse Transcriptase enzyme (Epicentre, USA) for 60 min at 50 °C in the presence of random hexamer primers. The sequence of primers for amplification of mouse TNF alpha is FWD 5′GAA AAG CAA GCA GCC AAC CA 3′ REV 5′ CGG ATC ATG CTT TCT GTG CTC 3′. PCR protocols have been published elsewhere (Garay et al., 2012). Cyclophilin *b* was chosen as a housekeeping gene based on the similarity of mRNA expression across all samples templates. Relative gene expression data were analyzed using the ABI PRISM 7500 sequence Detection System (Applied Biosystems, Foster City, CA, USA), calculated using the $2^{-\Delta\Delta ct}$ (Livak and Schmittgen, 2001) method and it was expressed as fold induction with respect to its corresponding control. Specificity of PCR amplification and the absence of dimers were confirmed by melting curve analysis. For amplification, 20 ng of cDNA was used and qPCR was performed under optimized conditions: 95 °C at 10 min followed by 40 cycles at 95 °C for 0.15 s and 60 °C for 1 min. Primers were used in a concentration of 0.2 μM.

2.9. Behavioral procedures

General considerations

Animals were tested during the light period, between 8:00 h and 14:00 h.The order of testing was as follows: open field (OF), elevated plus maze (EPM), novel object location recognition test (NOL) or Y maze exploration test, nest building test (NB) and tail suspension test (TST) with 1 week between each test, except for the OF and EPM that were carried within the same week, separated by 3 days. The ilummination density was approximately 50–100 lx at the center of the testing room.

2.9.1. Nest building test (NB)

Animals were single housed and provided with 16 pieces of $5 \times 5\,cm^2$ piled tissue paper in the front part of the cage. Twenty four hours later analysis of the built nest was done in a qualitative and quantitative manner. Qualitative assessment determined the presence or absence of a proper nest and a quantification of the torn paper was done, taking into account as torn, pieces of paper where the ripped surface exceeded $1\,cm^2$.

2.9.2. Novel object location recognition test (NOL)

NOL was performed as previously published (Beauquis et al., 2014). Locomotor activity, measured as total distance, was assessed in both trials (T1 and T2) with Any-maze video tracking system (Stoelting Co, USA).

2.9.3. Y maze

The Y-maze platform consisted of a black maze with three 30 cm arms in an equal angled disposition. Mice were adequately habituated to the room where the tests are carried out. The test consisted of two 10-min trials (sample trial or T1 and test trial or T2), separated by a 4-h inter-trial interval, that was recorded with a video camera. During T1, mice were allowed to explore two of the three arms, while during T2, the third novel arm exploration was permitted. Having verified that exploration in T1 was not different from the 50% in either arm, behavior in T2 was evaluated as the number of entries to the novel arm during the first two minutes of the test trial. Locomotor activity, measured as total distance as well as total entries, was assessed in both trials (T1 and T2) with Any-maze video tracking system (Stoelting Co, USA).

2.9.4. Elevated plus maze (EPM)

EPM consisted of four 30 cm arms, two open and two closed, elevated 50 cm high. After a 15 min adaptation to the testing room, mice were allowed to explore the maze during 10 min and recorded by a video camera. Upon video analysis, exploration time and entries to the open arms were quantified. Locomotor activity, measured as total distance, total entries and entries to closed arms were assessed with Any-maze video tracking system (Stoelting Co, USA).

2.9.5. Tail suspension test (TST)

Animals were tape-held by the tail to a 50 cm high frame and their activity was recorded during 6 min. Immobility time, considered when the animal was in a complete freezing state was measured using a chronometer.

2.9.6. Open field test (OF)

OF was carried out as previously published (Beauquis et al., 2014). Results are expressed as 'total distance traveled' as a measure of locomotion and 'percentage distance traveled in the center' in relation to total distance as a measure of anxious like behavior.

2.10. Statistical analysis

Data are expressed as mean +/− SEM. Analysis were performed under blind condition to the experimental groups. Statistical analysis were performed using unpaired one-tailed Student's *t*-test (for one sample or two independent samples) and two-way Anova or chi^2 test when required and were done using Prism 3.02 (GraphPad Software) and Infostat software (Universidad Nacional de Córdoba, Argentina). As regards the number of animals used for each determination, at least n = 4 animals were used for immunohistochemistry and western blot analysis (in 2–3 independent blots). For RT-qPCR and behavioral tests at least n = 7 animals were used and n = 4 for serum parameters (with a minimum of n = 8 for glycemia, insulinemia and pancreatic insulin measurements).

Table 1
Body weight and metabolic parameters at 2 and 5 months. Serum parameters and pancreatic insulin were determined after a 6-h fasting. (Student's t-test for independent samples, *p < 0.05, ** p < 0.01).

Parameter	CD	HFD
	5 months	
Final weight (g)	31.240 ± 0.46	30.23 ± 0.40
Glycemia (mg/dl)	142.10 ± 9.23	150.41 ± 6.15
Pancreatic insulin (ng/mg)	1.32 ± 0.19	1.74 ± 0.08*
Fasting insulin (ng/ml)	0.36 ± 0.01	0.42 ± 0.02*
HOMA	4.18 ± 0.41	4.84 ± 0.52
Triglycerides (mg/dl)	93.75 ± 9.72	86.50 ± 4.57
Cholesterol (mg/dl)	92.25 ± 14.45	142.75 ± 8.14*
c-HDL (mg/dl)	70.75 ± 14.07	109.75 ± 6.09*
PAF-AH (μmol/ml h)	33.04 ± 1.19	37.82 ± 095**
TNFα (pg/ml)	39.88 ± 5.70	38.12 ± 5.36
IL1b (pg/ml)	198.28 ± 64.62	247.7 ± 41.66
	2 months	
Final weight (g)	24.23 ± 0.52	23.97 ± 0.44
Glycemia (mg/dl)	177.10 ± 5.47	196.89 ± 7.63*
TNFα (pg/ml)	34.64 ± 2.44	38.96 ± 7.45
IL1b (pg/ml)	182.06 ± 84.50	1108.45 ± 319.64*

3. Results

3.1. High fat diet induces insulin resistance and dyslipidemia

At the end of the experiment, mice exposed to the high fat diet showed changes in several metabolic parameters but no differences were found regarding the body weight. In the subset of 2 month-old HFD, increased glycemia was found ($p < 0.05$ vs CD mice) but this change was not found in mice exposed to HFD for 4 months, when glycemia was slightly but not significantly increased in HFD mice compared to mice under standard diet. However, fasting insulinemia and pancreatic insulin content measured by RIA were higher in 5 month-HFD mice, suggestive of insulin resistance. Yet, the calculation of HOMA did not show differences between both groups. In relation to the lipid profile, whereas serum triglyceride levels exhibited no changes between experimental groups, cholesterol and cHDL- the most representative lipoprotein in rodents (Camus et al., 1983)—were found augmented in HFD mice serum respect to CD mice. Moreover, the activity of the proatherogenic LpPLA2 was increased in mice fed with the fat enriched diet ($p < 0.01$). Regarding to serum cytokine levels, at 2 months HFD mice exhibited a marked increase in IL-1β levels that were abolished at the end of the exposure (5 months), while TNFα levels remained unchanged in CD and HFD groups at both time points (Table 1).

3.2. Liver alterations. High fat diet is associated with increased hepatic lipid content, inflammation and diminished insulin signaling

H&E staining of paraffin embedded liver slices corresponding to HFD group revealed qualitatively elevated lipid content on hepatocytes compared to control group (Fig. 1B and C). The accumulation of lipids is evidenced by perinuclear white spaces left after the lipid washing upon tissue dehydration. When activated, insulin receptor autophosphorylates IRS1 and IRS2 ultimately promoting Akt activation, a central integrator of insulin signaling. Phosphorylation in serine residues in IRS is known to negatively modulate insulin signaling (Vadas et al., 2011). Evaluation of phosphorylated Akt levels is a well accepted manner to assess insulin resistance. To further characterize the effect of HFD in metabolism, we found that Akt phosphorylation in response to the induction with insulin, was diminished in mice exposed to the hyperlipidic diet, approximately at a 40% ($p < 0.01$), showing an impaired response (Fig. 1E). In line with this result, we found a twofold increase in the inhibitory phosphorylation of IRS1 ($p < 0.01$; Fig. 1F). Additionally, as a sign of hepatic HFD- induced inflammation, we found greater levels of TNFα mRNA expression in the RTqPCR assays (Fig. 1D, $p < 0.05$).

3.3. Nest building ability, short- and mid-term spatial memories are altered in C57Bl/6J mice exposed to a high fat diet

In order to assess the effect of HFD on mice cognitive status, we performed several behavioral tests related to relevant cerebral structures like hippocampus and amygdala. On the one hand, we evaluated nest building, a highly conserved ability associated to the performance of activities of daily living. For NB, mice were single housed during 24 h and provided with nesting material (Fig. 2A). The day after, we evaluated the position of the created nest (if any) and the grade of nesting material breakdown. As the image illustrates, CD mice mostly arranged the nest in the opposite side from where the nesting material was provided, coinciding with the darker part of the cage, as expected. In contrast, mice fed with the HFD failed to build a nest, as shown not only by the absence of a proper nest (Chi^2 test $p < 0.05$) but also by the diminished proportion of torn paper. Moreover, after the given time to carry out the test, the provided nesting material was frequently found untouched in cages corresponding to HFD mice.

Given the general alteration in behavior seen in this last test, we evaluated hippocampus-dependent spatial memory. Short-term spatial memory was evaluated by the Novel Object Location Recognition test (NOL). In Fig. 2B it can be observed that HFD group showed a poorer performance in this test, where the time exploring the relocated object was not statistically different from chance level (50%), suggesting a cognitive impairment involving short-term spatial memory. It is important to mention that, on the one hand, there were no differences in total distance traveled between groups in either trial (T1 or T2, $p = 0.44$ and $p = 0.67$, respectively) and on the other hand, mice did not show any preference for a particular object in T1 ($p = 0.17$ and $p = 0.18$ for CD and HFD exploration of one of the identical objects, respectively, comparing the relative exploration to 50%). Similarly, the number of entries to a novel arm was assessed in the Y maze exploration test and mice fed with the high fat diet showed again no differences with randomness, while control diet fed mice visited more frequently the novel arm, as expected. Again, here we found no differences in total distance traveled in either trial ($p = 0.58$ for T1 and $p = 0.71$ for T2). As we stated a 4 h period as inter-trial interval, the result could imply a potential alteration in the mid-term spatial memory (Fig. 2C).

3.4. High fat diet exposure induces alterations in emotional status: anxiety and depressive-like behavior

We explored certain emotional behavior aspects related to anxiety and depression. So as to evaluate the grade of an anxiety-related component in the behavioral profile, we performed the EPM test where the HFD group spent less time exploring the open arms ($p < 0.05$), more exposed and illuminated than closed ones, as Fig. 3A shows, whereas total entries as well as entries to closed arms did not differ between the groups ($p = 0.99$ and $p = 0.48$, respectively). This conduct is suggestive of an anxious- like perturbation. As regards the OF evaluation, no differences were found in total distance traveled, reinforcing the fact that the previously mentioned alterations are independent of locomotor capacity. Distance traveled in the center of the arena did not differ between the groups (Fig. 3C). However, the OF test is less specific than EPM in the assessment of anxiety. TST is a well accepted trial to measure depressive-like behavior, where immobilization time is associated to behavioral despair or a decreased effort in trying to escape. HFD mice exhibited a significant increase in this parameter in comparison to the control group (Fig. 3B, $p < 0.05$). We

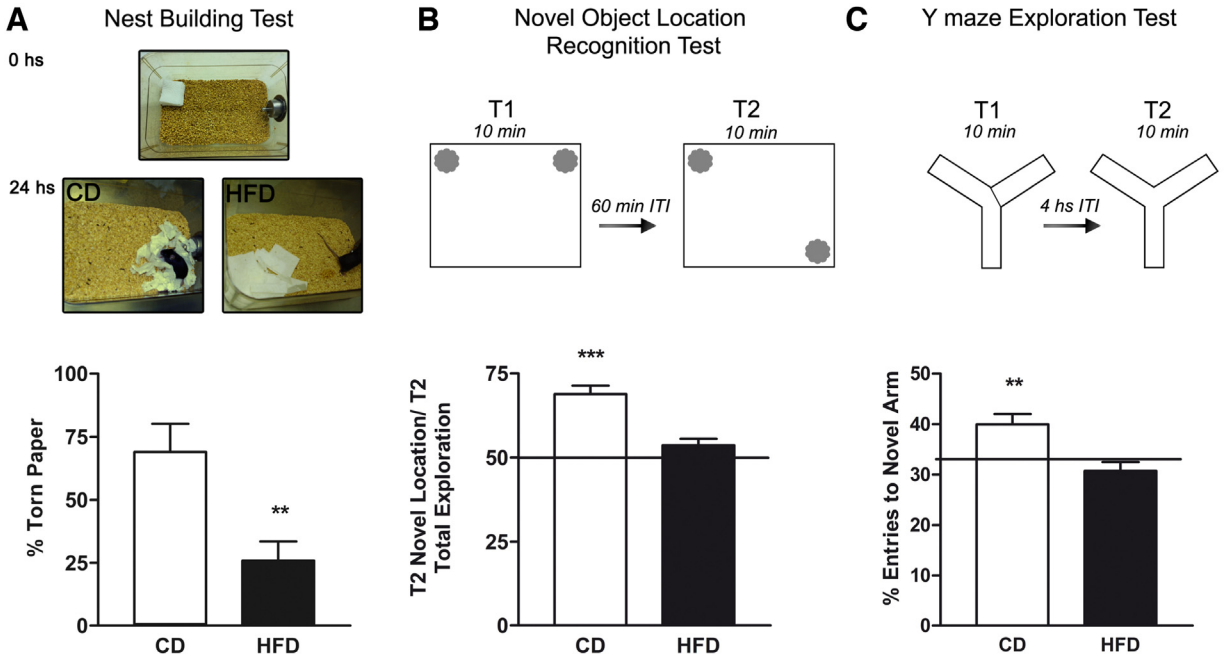

Fig. 2. Nest building behavior and spatial memory tasks. Panel A depicts qualitative (Chi^2 test $p < 0.05$) and quantitative assessment of nesting behavior (Student's *t*-test for independent samples, ** $p < 0.01$). The effect of HFD feeding on spatial memory was assessed by two different tasks: the novel object location recognition test, with a 1-h ITI (panel B) and the Y-maze exploration test, with a 4-h ITI (panel C). In both cases, exploration of the novel object location or the novel arm were compared to randomness (Student's *t*-test for one sample, ** $p < 0.01$, *** $p < 0.001$). For interpretation of the references to color in this figure legend, the reader is referred to the web version of the article.

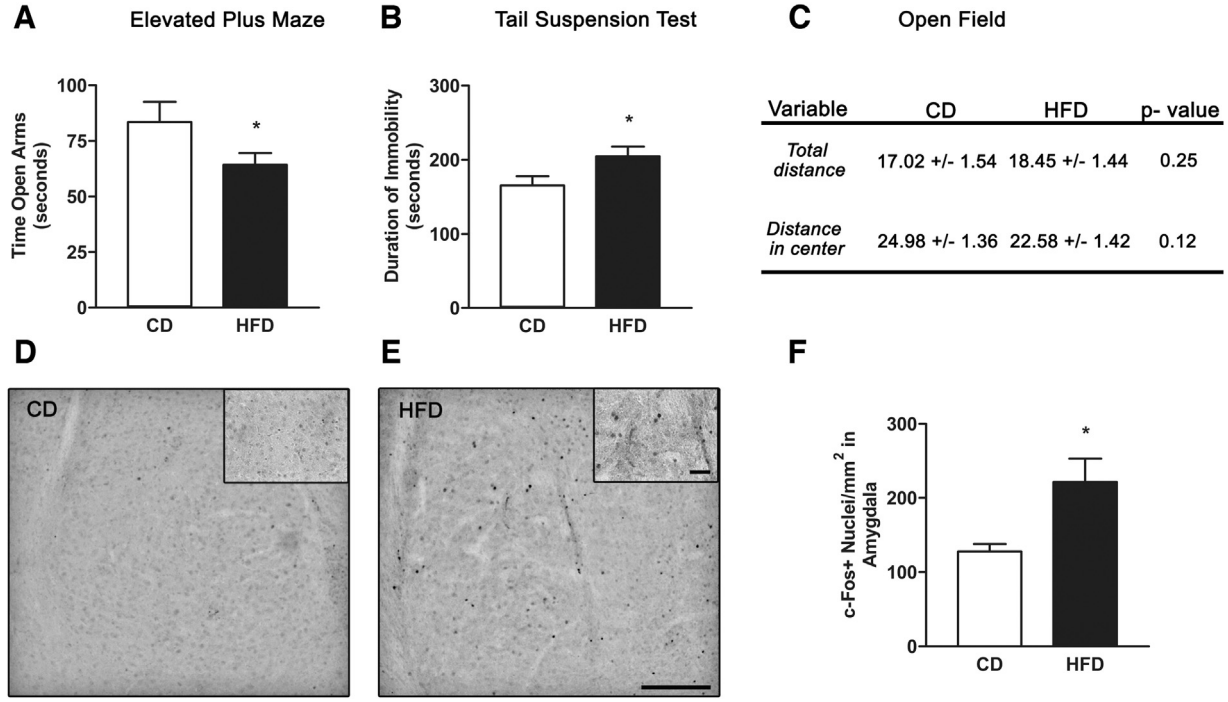

Fig. 3. Alterations in emotional behavior. Panel A shows the exploration time in the open arms of an elevated plus maze (EPM). Duration of immobility was assessed in the tail suspension test (B). In C, the table shows total distance and distance traveled in the center of an open field test. Panels D and E show representative 10× images of CD and HFD immunostained amygdala slices respectively (scale bar = 200 μm) with their respective 40× insets (scale bar = 50 μm) and panel F the corresponding quantification of c-Fos positive nuclei in central and basolateral amygdala. (Student's *t*-test for independent samples, * $p < 0.05$).

are able to conclude that the observed alterations are independent of impairment in locomotion or motivation to perform the tests, since locomotion was not altered in any of the apparatus used.

3.5. Increased c-Fos expression in amygdala after juvenile exposure to high fat diet, in concordance with behavioral changes

In relation to anxiety and depressive-like behavior results, we explored the potentially associated amygdaloid activity. Neu-

ronal activation was assessed by c-Fos+ cell counting in central and basolateral amygdaloid nuclei. A twofold increase was found in the number of positive c-Fos nuclei in mice exposed to HFD compared with CD, as it is shown in Fig. 3D–F. This amygdala hyperactivation could be associated with the emotional alterations induced by HFD, in terms of anxiety and depression, mentioned above.

3.6. High fat diet during juvenile period is linked to reduced adult neurogenesis in the hippocampal dentate gyrus

Proliferation capability in the GCL was studied by Ki67 immunolabeling on brain slices. The total number of Ki67+ cells decreased around 30% in mice exposed to HFD in comparison with normal fed group as it is shown in Fig. 4C. This diminished proliferation rate was seen irrespective of the hippocampal subregion analyzed, dorsal or ventral (Fig. 4E, two-way anova $p < 0.05$, significant diet effect).

As regards differentiation of newborn cells to neuronal linage in the DG, expression of DCX, marker of young neurons was examined. In this case, the dorsal hippocampal subregion from HFD mice specifically exhibited a lower number of DCX+ cells than CD mice ($p < 0.05$) while no differences were found in the ventral hippocampus (Fig. 4D and F). Representative images from Ki67 and DCX immunostaining are shown in Fig. 4A and B.

3.7. High fat diet induced insulin resistance in the hippocampus

In order to assess the brain ability to respond to insulin and a potential central insulin resistant state, as it was done in the liver, mice received 5UI/kgBW of insulin. Levels of phosphorylated Akt were found to be decreased by 37% in the hippocampus of HFD mice, (Fig. 4G, $p < 0.05$). Again, levels of the inhibitory phosphorylation of IRS1 in serine 636/639 were found to be increased in HFD mice (Fig. 4H, $p < 0.05$).

3.8. Inflammatory response in the hippocampus of HFD mice: increased microglial density and soma cell size

Microglial morphology was addressed in the hippocampus of CD and HFD rodents by immunohistochemistry against Iba1. Given recent results from our group identifying differential susceptibility to damage in particular hippocampal subfields (Pomilio et al., 2016), cell density was assessed in the stratum radiatum and the hilus of the dentate gyrus. The number of Iba1+ cell significantly increased 40% in the hilar region of HFD mice compared with the control group (Fig. 5A). In the stratum radiatum, we found a slight increment in cell density without reaching significance (Fig. 5C).

The soma size is a responsive parameter in microglia, associated to cellular activation. In both subfields of the hippocampus, an expansion in Iba1 somatic area was found in the HFD group, indicative of microglial activation ($p < 0.05$ and $p < 0.001$ for hilus and stratum radiatum, respectively; Fig. 5B and D). A representative image of Iba1 immustaining is shown in Fig. 5E.

The evaluation of the inflammatory response in the hippocampus included the detection of the prototypic pro inflammatory cytokines TNFα and IL-1β by ELISA and mRNA expression of TNFα by RT qPCR. Protein levels of TNFα and IL-1β did not differ between CD and HFD groups (Fig. 5F, table), and mRNA expression of TNFα was not found to be altered either ($1.03 +/- 0.09$ vs $1.19 +/- 0.13$ relative levels of TNFα mRNA in CD and HFD groups respectively $p = 0.16$).

4. Discussion

Besides clinical and epidemiological evidence, several scientific groups working on basic neuroscience with rodents addressed the impact of high fat diets on the brain, stressing the magnitude and relevance of this topic (Boitard et al., 2012; Freeman et al., 2014; Sobesky et al., 2014; Vendruscolo et al., 2010). However, the variability in mice strains used, the diversity of administered diets and the time window when the animals are exposed to the diet provide important heterogeneity to the discussion of obtained results.

Our work examines the neurological effects of a moderately high fat diet consumed during the critical juvenile period of life in rodents. This age coincides with crucial biological events as body growth, hormonal changes, cerebral maturation and establishment of brain circuits (Spear, 2000) featuring a highly vulnerable time window to environmental and endogenous stressors.

The high fat diet administered to C57BL/6J male mice during 4 months was able to induce hyperinsulinemia, increased insulin production and dyslipidemia without an impact on body weight or blood glucose. In addition, HFD caused hepatic lipid accumulation and inflammation contributing to decreased insulin signaling in this tissue. This finding in the liver together with the high levels of serum and pancreatic insulin is suggestive of insulin resistance. Diminished insulin signaling was also verified in the hippocampus of HDF mice. Moreover, this diet promoted an inflammatory and prothrombotic context evidenced by the increased activity of the plasmatic enzyme LpPLA2, associated to cardiovascular risk.

Cognitive performance and emotionality were significantly perturbed after the exposure to this diet. We found that HFD fed mice exhibited impairment in nest building compared with CD. To our knowledge, this is the first report showing alterations in NB behavior in rodents exposed to a high fat diet. Interestingly, nesting behavior is displayed by both males and females in parental and non-parental contexts and it is considered a cognitively flexible behavior, mainly controlled by levels of arousal and motivation (Wesson and Wilson, 2011). Impairment in nest building has been found in mice with hippocampus lesions and, among other typical behaviors such as burrowing and hoarding are thought as reminiscent of the impairments in activities of daily living (ADL) so characteristic of AD (Filali and Lalonde, 2009; Deacon, 2012; Deacon et al., 2015). Hence, our results suggest an early-life disruption in motivated behavior, indicative of cognitive dysfunction that could be associated to impairments in activities of daily living as it occurs early in AD.

Short and mid-term spatial memories were also disturbed as a consequence of the high fat diet. Spatial memory strongly depends on the integrity of the hippocampus. The dorsal and ventral hippocampi have been suggested to be functionally distinct structures (Moser and Moser, 1998; Fanselow and Dong, 2010). While spatial and contextual memories are associated with the dorsal hippocampus, ventral lesions alter stress-related responses (Henke, 1990). Evidence including specific ventral and/or dorsal hippocampal lesions well demonstrated the correlation with a poor performance in spatial memory tasks (Broadbent et al., 2004). Our results showing a reduced performance in the NOL and the Y maze suggest spatial memory dysfunction in mice exposed to HFD.

Neurogenesis in the SGZ of the dentate gyrus is certainly a key process involved not only in the cognitive status, memory acquisition and learning ability, but in the emotional status, anxiety and depressive-like behaviors (Boitard et al., 2015; Papazoglou et al., 2015). We found a generalized decrease of cell proliferation in the dentate gyrus of HFD mice, assessed as Ki67+ cells throughout the entire hippocampus. Neuronal differentiation was found specifically perturbed on the dorsal hippocampus, with less number of DCX+ immature neurons, potentially underlying the spatial memory dysfunction found in mice exposed to HFD. Interestingly, low

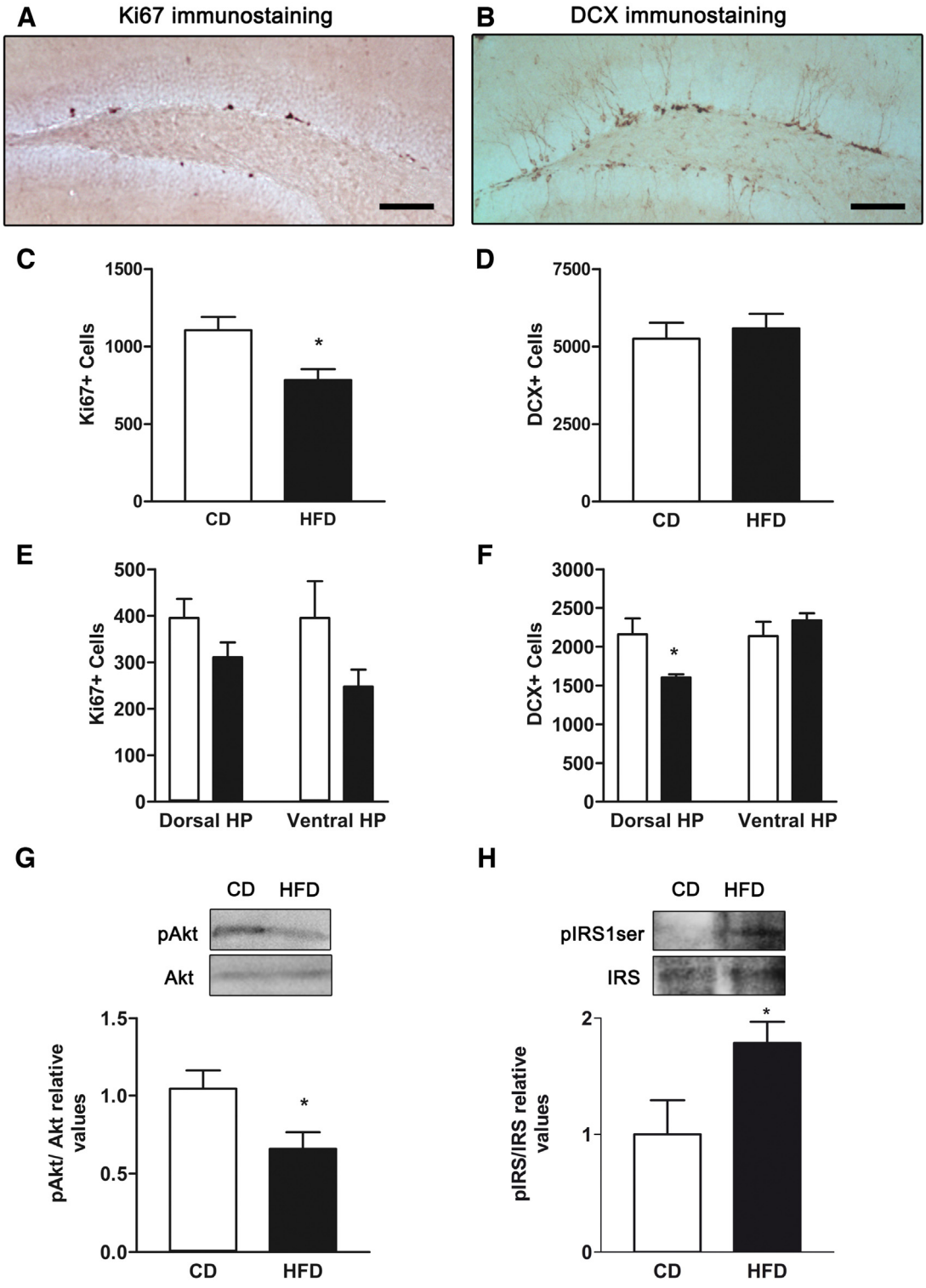

Fig. 4. Neurogenic capability and insulin sensitivity in the hippocampus of mice exposed to HFD diet. Proliferation in the subgranular zone of the dentate gyrus was assessed. In A, a 10× representative photograph of Ki67 (scale bar = 100 μm) immunoreactivity is shown and the quantification of Ki67 positive cells across the entire dentate gyrus (panel C Student's *t*-test for independent samples, * $p < 0.05$) as well as discriminated into dorsal and ventral hippocampus in E (Two-way Anova * $p < 0.05$). In B, a 10× representative image of DCX immunostaining is shown (scale bar = 100 μm), together with the quantification of DCX positive cells in the granular cell layer of whole hippocampus (panel D, Student's *t*-test for independent samples, non-significant) or dorsal and ventral hippocampus (panel F, Two-way Anova followed by orthogonal contrasts * $p < 0.05$). Assessment of Insulin signaling was done by western blot analysis from hemi-hippocampal homogenates. Panel G shows representative bands from pAkt and Akt blot and their corresponding densitometry analyses and panel H shows representative bands from IRS1 and its inhibitory phosphorylation followed by their corresponding densitometry analysis. (Student's *t*-test for independent samples, * $p < 0.05$). For interpretation of the references to color in this figure legend, the reader is referred to the web version of the article.

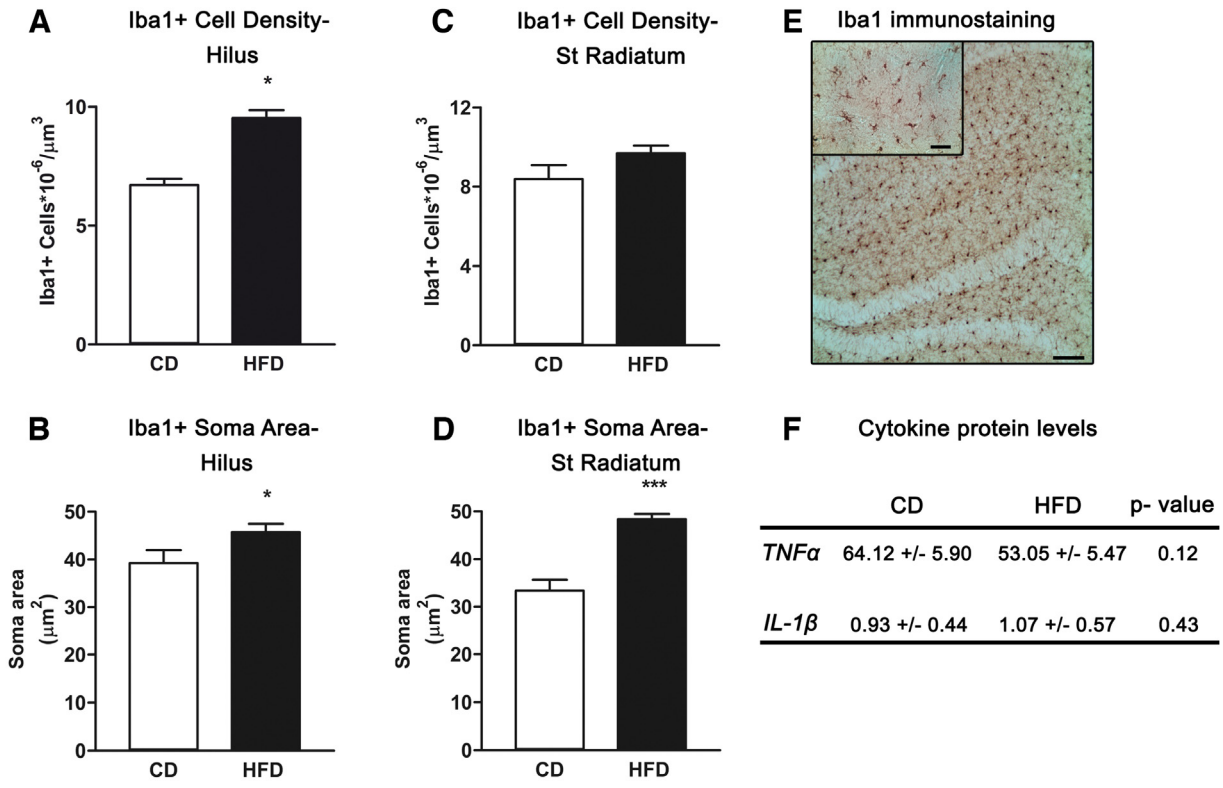

Fig. 5. Microglial alterations in the hippocampus of HFD mice. The number of microglial Iba1+ cells and Iba1+ cells soma area in the hilar subfield of the hippocampus are shown in panel A and B, respectively. Panels C and D show the same parameters measured in stratum radiatum subregion. A 10× representative Iba1 immunostaining image (scale bar = 100 μm) with a 40× inset (scale bar = 20 μm) is shown in E. In F, the table shows protein levels of the cytokines TNFα and IL1b measured by ELISA in hippocampal homogenates. (Student's t-test for independent samples, * $p < 0.05$, *** $p < 0.001$). For interpretation of the references to color in this figure legend, the reader is referred to the web version of the article.

neurogenesis in the dentate gyrus is associated with aging (Saravia et al., 2007), neurodegenerative disorders (Beauquis et al., 2008) and specifically with some psychiatric conditions like depression (Tanti and Belzung, 2013).

The exposure to HFD also promoted an altered emotional phenotype involving anxiety and depressive-like behavior. In line with these results, we detected elevated neural activity in the amygdala. The amygdala is recognized as a prominent actor in the complex regulation of the stress response and emotional control of behavior, in close connection with the hippocampus. Recent studies explored the impact of metabolic disorders during juvenile period on the functionality of this brain region (Boitard et al., 2015). Our results showing the anxiety increase, depressive-like behavior and amygdaloid activation emphasize the involvement of emotionality in metabolic dysfunction linked to HFD consumption during the peri-adolescent period.

Inflammation is an important phenomenon in a plethora of pathological conditions and cytokines and chemokines have a variety of detrimental effects in the physiology of the brain at different levels, affecting behavior, neurogenesis, BDNF expression and microglia activation, among others (Russo et al., 2011; Freeman et al., 2014). Furthermore, cytokines and stress kinases JNK, IKK and PKR play a key role in the development of insulin resistance, affecting relevant processes that involve cell homeostasis, viability and synaptic plasticity (Bomfim et al., 2012; de la Monte and Tong, 2014). Our results show that at shorter exposure to HFD (2 month-old mice), serum levels of IL1β levels were markedly increased together with elevated glycemia. However, at the end of the exposure (5 months) these two parameters did not differ from control group insinuating the existence of compensatory phenomena to an acute and transitory response.

Interestingly, TNFα and IL1β levels were not found to be increased neither in serum nor in hippocampus of 5 month-old HFD mice, unlike other reports state in the literature (Miller and Spencer, 2014). In line with our results, Boitard and co-workers suggested the notion that cytokine production induced by HFD could only be exacerbated by the presence of an immune challenge such as LPS, acting as a second "hit" (Boitard et al., 2014). Our data suggest a time dependent- IL1β response dynamics; with an early increase of this cytokine in plasma that could initiate the inflammatory response in both, the periphery and the CNS.

Lastly, we cannot exclude the involvement of leptin and related receptors, as it was suggested by Del Olmo group, studying the HFD effect on adolescent mice (Valladolid-Acebes et al., 2013) or alternative mechanisms to inflammation underlying the observed CNS alterations. For instance, free fatty acids are known to contribute to the lipid toxicity in HFD paradigms. A single palmitic acid injection has shown to have a direct effect on dopamine and serotonin metabolism in the hippocampus and amygdala of mice, suggesting the participation of alternative metabotropic pathways as the free fatty acid receptors and independently of the canonical toll-like receptor 4 (TLR4) inflammatory response (Moon et al., 2014). Moreover, lipoproteins that we found here increased after a fat diet as well as advanced glycation end products and oxidized lipoproteins augmented in rich fat diet reported by Velloso and coworkers (Velloso et al., 2015) could act directly on TLRs or on alternative sites promoting neuronal and/or glial changes. Besides, it is well characterized that rodent models of obesity, T2D or metabolic syndrome exhibit an altered hypothalamic-pituitary-adrenal axis that could account for a maladapted response to stress, sickness behavior and associated disorders (Beauquis et al., 2010; Grillo et al., 2014).

Physiologically, in an intact brain, ramified microglia is essential in establishing a successful neurogenic niche, promoting neural stem cells proliferation, differentiation and survival (Santos et al., 2015). Our work depicts that HFD induced alterations compatible with an increase of microglial activation in the hilus of the dentate gyrus suggesting both a loss-of-function phenotype regarding the supporting role of ramified microglia in the neurogenic process and a gain-of-function phenotype in relation to the detrimental effects of the proinflammatory profile of reactive microglia. These results were associated to diminished proliferation in the SGZ together with an impaired neuronal differentiation in the dorsal hippocampus. Interestingly, emerging data is linking microglia dysfunction with psychiatric conditions. Deviation from microglial homeostasis occurs in neurodegenerative diseases associated to aging or during inflammatory process as a consequence of stress, infections or stroke, all converging in depression (Yirmiya et al., 2015).

Microglial activation in the hippocampus could play a critical role linking metabolic and neurological changes and deserves further investigation.

5. Conclusion

Our study supports the association between metabolic dysfunction induced by fat diet intake during the juvenile period and cognitive and emotional perturbations including anxious- and depressive-like behaviors. We show that metabolic and neurological alterations are relevant even in absence of obesity and overt diabetes. Early life period appears to be particularly vulnerable to the detrimental effects of HFD consumption on limbic functioning at both behavioral and cellular levels at the adult age.

Conflict of interest

The authors declare that no competing interests exist.

Role of founding source

This work was supported by a grant to JB from Alberto Roemmers Foundation and Agencia Nacional de Promoción de Ciencia y Tecnología of Argentina (ANPCyT) PICT 2013- #2645 and to FS from ANPCyT PICT 2011 #1012 2014#1168; PIP CONICET 2013–2015 N° 473 and Fundación René Barón.

Contributors

Conceived and designed the experiments: AV, JB & FS. Performed the experiments: AV Analyzed the data: AV, CP & JB. Contributed reagents/materials/analysis tools: CP, MM, MMB, LG, MFM RS; VLL & FB. Wrote the paper: AV, JB & FS.

Acknowledgements

The authors deeply thank Maria Eugenia Matzkin, Soledad Rossi and Monica Frungieri; for their kind collaboration and RT PCR expertise; Julio Bernal for chow preparation and the personnel of the animal facility at the Instituto de Biología y Medicina Experimental (IBYME) for their help with animal care. JB, FB LG VLL RS and FS are career investigators from Consejo Nacional de Investigaciones Científicas y Técnicas of Argentina (CONICET). AV and CP are doctoral fellows from CONICET.

References

Andersen, S.L., 2003. Trajectories of brain development: point of vulnerability or window of opportunity? Neurosci. Biobehav. Rev. 27, 3–18.

Beauquis, J., Roig, P., Homo-Delarche, F., De Nicola, A., Saravia, F., 2006. Reduced hippocampal neurogenesis and number of hilar neurones in streptozotocin-induced diabetic mice: reversion by antidepressant treatment. Eur. J. Neurosci. 23, 1539–1546.

Beauquis, J., Saravia, F., Coulaud, J., Roig, P., Dardenne, M., Homo-Delarche, F., De Nicola, A., 2008. Prominently decreased hippocampal neurogenesis in a spontaneous model of type 1 diabetes, the nonobese diabetic mouse. Exp. Neurol. 210, 359–367.

Beauquis, J., Homo-Delarche, F., Giroix, M.H., Ehses, J., Coulaud, J., Roig, P., Portha, B., De Nicola, A.F., Saravia, F., 2010. Hippocampal neurovascular and hypothalamic–pituitary–adrenal axis alterations in spontaneously type 2 diabetic GK rats. Exp. Neurol. 222, 125–134.

Beauquis, J., Vinuesa, A., Pomilio, C., Pavia, P., Galvan, V., Saravia, F., 2014. Neuronal and glial alterations, increased anxiety, and cognitive impairment before hippocampal amyloid deposition in PDAPP mice, model of Alzheimer's disease. Hippocampus 24, 257–269.

Biessels, G., Kappelle, A., Bravenboer, B., Gispen, W., 1994. Cerebral function in diabetes mellitus. Diabetologia 37, 643–650.

Blank, M.L., Hall, M.N., Cress, E.A., Snyder, F., 1983. Inactivation of 1-alkyl-2-acetyl-sn-glycero-3-phosphocholine by a plasma acetylhydrolase: higher activities in hypertensive rats. Biochem. Biophys. Res. Commun. 113, 666–671.

Boitard, C., Etchamendy, N., Sauvant, J., Aubert, A., Tronel, S., Marighetto, A., Laye, S., Ferreira, G., 2012. Juvenile, but not adult exposure to high-fat diet impairs relational memory and hippocampal neurogenesis in mice. Hippocampus 22, 2095–2100.

Boitard, C., Cavaroc, A., Sauvant, J., Aubert, A., Castanon, N., Laye, S., Ferreira, G., 2014. Impairment of hippocampal-dependent memory induced by juvenile high-fat diet intake is associated with enhanced hippocampal inflammation in rats. Brain Behav. Immun. 40, 9–17.

Boitard, C., Maroun, M., Tantot, F., Cavaroc, A., Sauvant, J., Marchand, A., Laye, S., Capuron, L., Darnaudery, M., Castanon, N., Coutureau, E., Vouimba, R.M., Ferreira, G., 2015. Juvenile obesity enhances emotional memory and amygdala plasticity through glucocorticoids. J. Neurosci. 35, 4092–4103.

Bomfim, T.R., Forny-Germano, L., Sathler, L.B., Brito-Moreira, J., Houzel, J.C., Decker, H., Silverman, M.A., Kazi, H., Melo, H.M., McClean, P.L., Holscher, C., Arnold, S.E., Talbot, K., Klein, W.L., Munoz, D.P., Munoz, D.P., De Felice, F.G., 2012. An anti-diabetes agent protects the mouse brain from defective insulin signaling caused by Alzheimer's disease—associated Abeta oligomers. J. Clin. Invest. 122, 1339–1353.

Bonaventura, M.M., Catalano, P.N., Chamson-Reig, A., Arany, E., Hill, D., Bettler, B., Saravia, F., Libertun, C., Lux-Lantos, V.A., 2008. GABAB receptors and glucose homeostasis: evaluation in GABAB receptor knockout mice. Am. J. Physiol. Endocrinol. Metab. 294, E157–E167.

Bradford, M.M., 1976. A rapid and sensitive method for the quantitation of microgram quantities of protein utilizing the principle of protein-dye binding. Anal. Biochem. 7, 248–254.

Broadbent, N.J., Squire, L.R., Clark, R.E., 2004. Spatial memory, recognition memory, and the hippocampus. Proc. Natl. Acad. Sci. U. S. A. 101, 14515–14520.

Calvo-Ochoa, E., Arias, C., 2015. Cellular and metabolic alterations in the hippocampus caused by insulin signaling dysfunction and its association with cognitive impairment during aging and Alzheimer's disease: studies in animal models. Diabetes Metab. Res. Rev. 31, 1–13.

Camus, M.C., Chapman, M.J., Forgez, P., Laplaud, P.M., 1983. Distribution and characterization of the serum lipoproteins and apoproteins in the mouse, Mus musculus. J. Lipid Res. 24, 1210–1228.

Castanon, N., Luheshi, G., Laye, S., 2015. Role of neuroinflammation in the emotional and cognitive alterations displayed by animal models of obesity. Front. Neurosci. 9, 229.

Deacon, R.M., Altimiras, F.J., Bazan-Leon, E.A., Pyarasani, R.D., Nachtigall, F.M., Santos, L.S., Tsolaki, A.G., Pednekar, L., Kishore, U., Biekofsky, R.R., Vasquez, R.A., Cogram, P., 2015. Natural AD-Like neuropathology in octodon degus: impaired burrowing and neuroinflammation. Curr. Alzheimer Res. 12, 314–322.

Deacon, R., 2012. Assessing burrowing, nest construction, and hoarding in mice. J. Vis. Exp., e2607.

Dineley, K.T., Jahrling, J.B., Denner, L., 2014. Insulin resistance in Alzheimer's disease. Neurobiol. Dis. 72 (Pt. A), 92–103.

de la Monte, S.M., Tong, M., 2014. Brain metabolic dysfunction at the core of Alzheimer's disease. Biochem. Pharmacol. 88, 548–559.

Fanselow, M.S., Dong, H.W., 2010. Are the dorsal and ventral hippocampus functionally distinct structures? Neuron 65, 7–19.

Fehm, H.L., Kern, W., Peters, A., 2006. The selfish brain: competition for energy resources. Prog. Brain Res. 153, 129–140.

Filali, M., Lalonde, R., 2009. Age-related cognitive decline and nesting behavior in an APPswe/PS1 bigenic model of Alzheimer's disease. Brain Res. 1292, 93–99.

Freeman, L.R., Haley-Zitlin, V., Rosenberger, D.S., Granholm, A.C., 2014. Damaging effects of a high-fat diet to the brain and cognition: a review of proposed mechanisms. Nutr. Neurosci. 17, 241–251.

Garay, L.I., Gonzalez Deniselle, M.C., Brocca, M.E., Lima, A., Roig, P., De Nicola, A.F., 2012. Progesterone down-regulates spinal cord inflammatory mediators and increases myelination in experimental autoimmune encephalomyelitis. Neuroscience 226, 40–50.

Grillo, C.A., Mulder, P., Macht, V.A., Kaigler, K.F., Wilson, S.P., Wilson, M.A., Reagan, L.P., 2014. Dietary restriction reverses obesity-induced anhedonia. Physiol. Behav. 128, 126–132.

Henke, P.G., 1990. Limbic system modulation of stress ulcer development. Ann. N. Y. Acad. Sci. 597, 201–206.
LeDoux, J., 2003. The emotional brain, fear, and the amygdala. Cell. Mol. Neurobiol. 23, 727–738.
Livak, K.J., Schmittgen, T.D., 2001. Analysis of relative gene expression data using real-time quantitative PCR and the 2(-Delta Delta C(T)) Method. Methods 25, 402–408.
Maren, S., 2005. Synaptic mechanisms of associative memory in the amygdala. Neuron 47, 783–786.
Miller, A.A., Spencer, S.J., 2014. Obesity and neuroinflammation: a pathway to cognitive impairment. Brain Behav. Immun. 42, 10–21.
Moll, L., Schubert, M., 2012. The role of insulin and insulin-like growth factor-1/FoxO-mediated transcription for the pathogenesis of obesity-associated dementia. Curr. Gerontol. Geriatr. Res. 2012, 384094.
Moon, M.L., Joesting, J.J., Lawson, M.A., Chiu, G.S., Blevins, N.A., Kwakwa, K.A., Freund, G.G., 2014. The saturated fatty acid, palmitic acid, induces anxiety-like behavior in mice. Metabolism 63, 1131–1140.
Moser, M.B., Moser, E.I., 1998. Distributed encoding and retrieval of spatial memory in the hippocampus. J. Neurosci. 18, 7535–7542.
Muzzio, M.L., Miksztowicz, V., Brites, F., Aguilar, D., Repetto, E.M., Wikinski, R., Tavella, M., Schreier, L., Berg, G.A., 2009. Metalloproteases 2 and 9: Lp-PLA(2) and lipoprotein profile in coronary patients. Arch. Med. Res. 40, 48–53.
Papazoglou, I.K., Jean, A., Gertler, A., Taouis, M., Vacher, C.M., 2015. Hippocampal GSK3beta as a molecular link between obesity and depression. Mol. Neurobiol. 52, 363–374.
Pomilio, C., Pavia, P., Gorojod, R.M., Vinuesa, A., Alaimo, A., Galvan, V., Kotler, M.L., Beauquis, J., Saravia, F., 2016. Glial alterations from early to late stages in a model of Alzheimer's disease: evidence of autophagy involvement in Abeta internalization. Hippocampus 26, 194–210.
Puder, J.J., Munsch, S., 2010. Psychological correlates of childhood obesity. Int. J. Obes. (Lond.) 34 (Suppl. 2), S37–S43.
Russo, I., Barlati, S., Bosetti, F., 2011. Effects of neuroinflammation on the regenerative capacity of brain stem cells. J. Neurochem. 116, 947–956.
Santos, L.E., Beckman, D., Ferreira, S.T., 2015. Microglial dysfunction connects depression and Alzheimer's disease. Brain Behav. Immun., 30056–30058, http://dx.doi.org/10.1016/j.bbi.11.011, pii: S0889-1591(15) [Epubaheadofprint].
Saravia, F., Beauquis, J., Pietranera, L., De Nicola, A.F., 2007. Neuroprotective effects of estradiol in hippocampal neurons and glia of middle age mice. Psychoneuroendocrinology 32, 480–492.
Sobesky, J.L., Barrientos, R.M., De May, H.S., Thompson, B.M., Weber, M.D., Watkins, L.R., Maier, S.F., 2014. High-fat diet consumption disrupts memory and primes elevations in hippocampal IL-1beta, an effect that can be prevented with dietary reversal or IL-1 receptor antagonism. Brain Behav. Immun. 42, 22–32.
Spear, L.P., 2000. The adolescent brain and age-related behavioral manifestations. Neurosci. Biobehav. Rev. 24, 417–463.
Stranahan, A.M., Arumugam, T.V., Cutler, R.G., Lee, K., Egan, J.M., Mattson, M.P., 2008. Diabetes impairs hippocampal function through glucocorticoid-mediated effects on new and mature neurons. Nat. Neurosci. 11, 309–317.
Tanti, A., Belzung, C., 2013. Hippocampal neurogenesis: a biomarker for depression or antidepressant effects? Methodological considerations and perspectives for future research. Cell Tissue Res. 354, 203–219.
Vadas, O., Burke, J.E., Zhang, X., Berndt, A., Williams, R.L., 2011. Structural basis for activation and inhibition of class I phosphoinositide 3-kinases. Sci. Signal. 4, re2.
Valdivia, S., Patrone, A., Reynaldo, M., Perello, M., 2014. Acute high fat diet consumption activates the mesolimbic circuit and requires orexin signaling in a mouse model. PLoS One 9, e87478.
Valladolid-Acebes, I., Fole, A., Martin, M., Morales, L., Cano, M.V., Ruiz-Gayo, M., Del Olmo, N., 2013. Spatial memory impairment and changes in hippocampal morphology are triggered by high-fat diets in adolescent mice. Is there a role of leptin? Neurobiol. Learn. Mem. 106, 18–25.
Velloso, L.A., Folli, F., Saad, M.J., 2015. TLR4 at the crossroads of nutrients, gut microbiota, and metabolic inflammation. Endocr. Rev. 36, 245–271.
Vendruscolo, L.F., Gueye, A.B., Darnaudery, M., Ahmed, S.H., Cador, M., 2010. Sugar overconsumption during adolescence selectively alters motivation and reward function in adult rats. PLoS One 5, e9296.
WHO, http://www.who.int/dietphysicalactivity/childhood, 2015.
Wesson, D.W., Wilson, D.A., 2011. Age and gene overexpression interact to abolish nesting behavior in Tg2576 amyloid precursor protein (APP) mice. Behav. Brain Res. 216, 408–413.
Yirmiya, R., Rimmerman, N., Reshef, R., 2015. Depression as a microglial disease. Trends Neurosci. 38, 637–658.